

## Supplementary Information

### Single-Ion Polymer/LLZO Hybrid Electrolytes with High Lithium Conductivity

Marine Lechartier,<sup>a,b</sup> Luca Porcarelli,<sup>a,c</sup> Haijin Zhu,<sup>c</sup> Maria Forsyth,<sup>a,c,d</sup> Aurélie Guéguen,<sup>b</sup> Laurent Castro\*<sup>b</sup> and David Mecerreyes\*<sup>c,d</sup>

<sup>a</sup> POLYMAT University of the Basque Country UPV/EHU, Avenida Tolosa 72, Donostia-San Sebastian 2008, Spain.

<sup>b</sup> Toyota Motor Europe Research & Development 1, Advanced Material Research, Battery & Fuel Cell, Hoge Wei 33 B, B-1930 Zaventem, Belgium

<sup>c</sup> ARC Centre of Excellence for Electromaterials Science and Institute for Frontier Materials, Deakin University, Melbourne, Australia

<sup>d</sup> Ikerbasque, Basque Foundation for Science, E-48011, Bilbao, Spain.

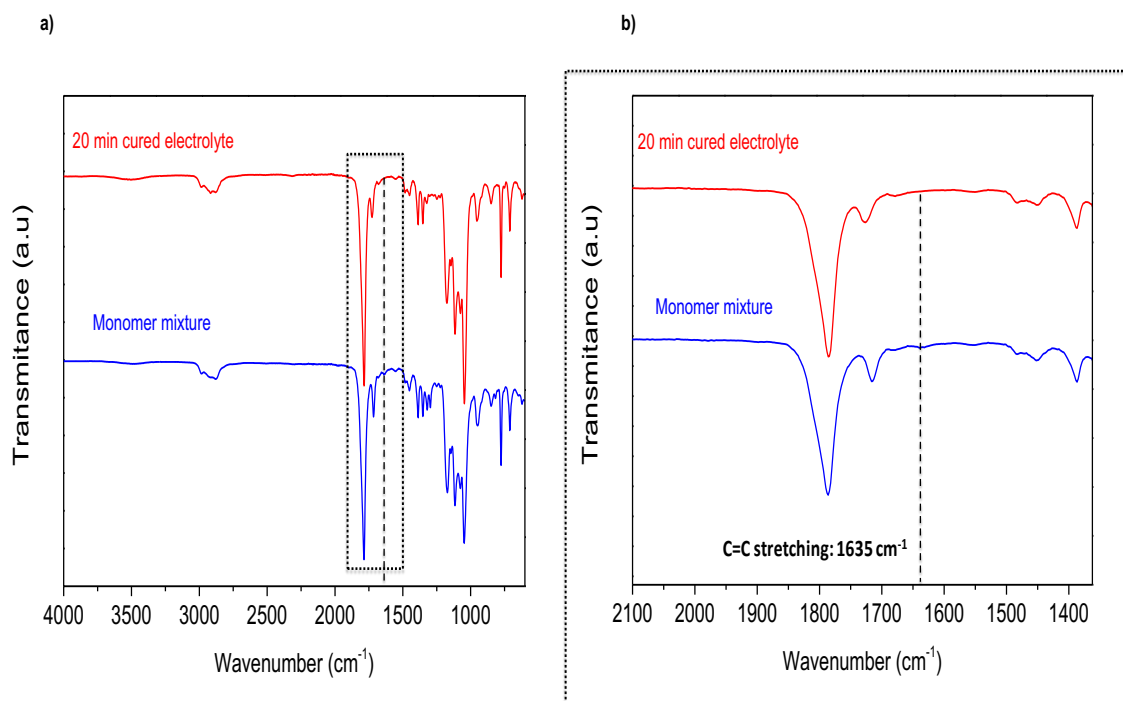


Fig.S1. (a) FTIR spectra of monomers mixture and 20 min cured SIPE  
(b) Zoom to show the disappearance of C=C stretching band after curing

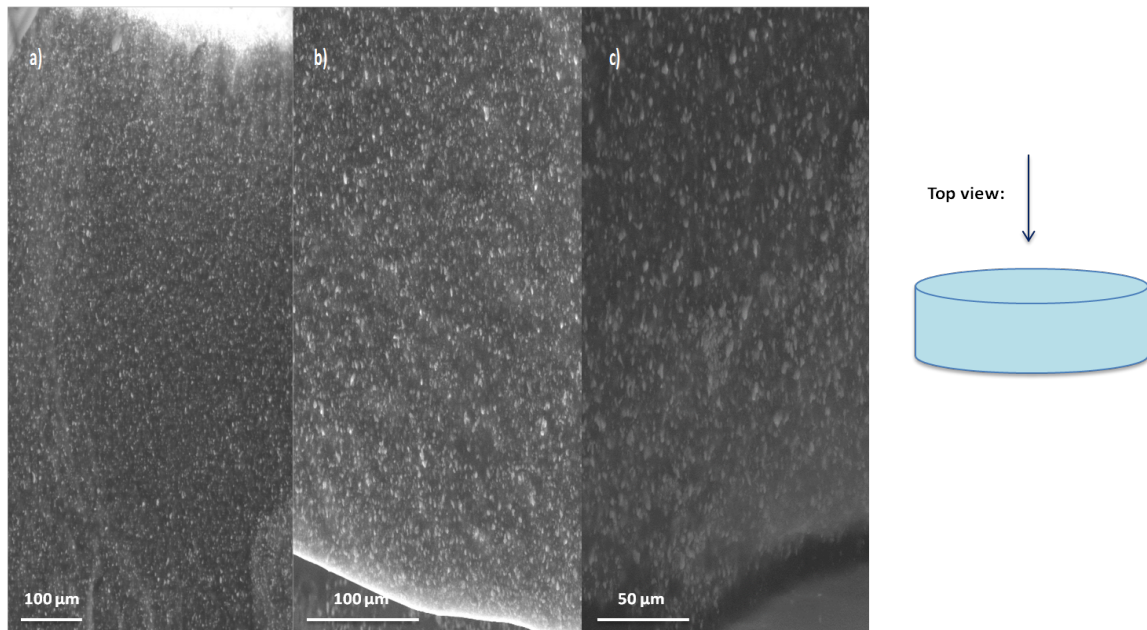


Fig.S2. ESEM pictures on top view of single ion hybrid crosslinked polymers:  
(a) HSIPE-26, (b) HSIPE-40, (c) HSIPE-50

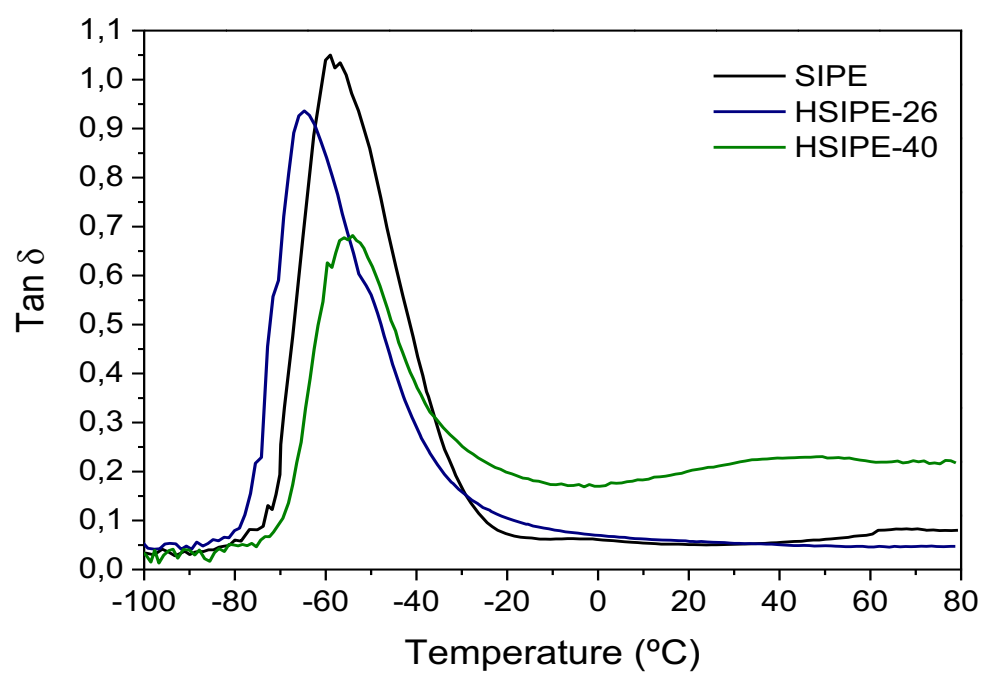


Fig.S3. Tan ( $\delta$ ) in function of temperature for pristine and hybrid single ion crosslinked polymer electrolytes

**Table S4:** Comparison of different LLZO hybrid polymers in terms of ionic conductivity and galvanostatic cycling

Authors	Matrix	Li salt	Composition	Ionic conductivity (S.cm <sup>-1</sup> )	Li/Li galvanostatic cycling
Our study	Single ion crosslinked polymer	Salt free	26 wt.%	$1,17.10^{-4}$ (25 °C)	At 60°C: Without short circuit -0.1 mA.cm <sup>-2</sup> for 6h, -0.25 mA.cm <sup>-2</sup> for 6h, -0.5 mA.cm <sup>-2</sup> for 6h, -1 mA.cm <sup>-2</sup> for 6h With short circuit -2 mA.cm <sup>-2</sup> for 6h, -4 mA.cm <sup>-2</sup> for 6h
Huo & al [1]	PEO	Salt free	15 vol.%	$2,2.10^{-4}$ (25 °C)	At 30°C: - 0.5 mA.cm <sup>-2</sup> for 7500 min - 1 mA.cm <sup>-2</sup> for 500 min before short circuit
Choi & al [2]	PEO	LiClO <sub>4</sub>	52.5 wt.%	$4,42.10^{-4}$ (55 °C)	-
Zhang & al [3]	PEO	Salt free	12.7 vol.%	$2,1.10^{-4}$ (30 °C)	At 60°C: - 3 mA.cm <sup>-2</sup> over 750h without short circuit. When LiTFSI is added, short circuit over 25h cycling
Chen & al [4]	PEO	LiTFSI	7.5 wt.%	$5,5.10^{-4}$ (25 °C)	At 60°C: - 0.2 mA.h.cm <sup>-2</sup> over 15h
Zheng & al [5]	PEO/ TEGDME	LiClO <sub>4</sub>	40 wt.%	$4.10^{-5}$ (25 °C)	-
Keller & al [6]	PEO	LiTFSI	70 wt.%	$\approx 10^{-5}$ (25 °C)	At 60°C: - 5 μA.cm <sup>-2</sup> for 20h - 10 μA.cm <sup>-2</sup> for 10h - 20 μA.cm <sup>-2</sup> for 5h - 50 μA.cm <sup>-2</sup> for 2h - 100 μA.cm <sup>-2</sup> for 1h
Langer & al [7]	PEO	LiClO <sub>4</sub>	40 wt.%	$5.10^{-5}$ (80 °C)	-

Cheng & al [8]	PEO	LiClO <sub>4</sub>	30 wt.%	$3,1 \cdot 10^{-6}$ (25°C)	-
Zagórski & al [9]	PEO	LiTFSI	10 vol.% (31 wt.%)	$4,5 \cdot 10^{-4}$ (70°C)	At 70°C - 0.1 mA.cm <sup>-2</sup> for 2h For PEO-LiTFSI, short circuit over 88h cycling For PEO-LiTFSI-LLZO, cycling over 750h but voltage instabilities (first 70h)

References:

- [1] H. Huo, N. Zhao, J. Sun, F. Du, Y. Li, X. Guo, Composite electrolytes of polyethylene oxides/garnets interfacially wetted by ionic liquid for room-temperature solid-state lithium battery, *J. Power Sources*. 372 (2017) 1–7. <https://doi.org/10.1016/j.jpowsour.2017.10.059>.
- [2] J.-H. Choi, C.-H. Lee, J.-H. Yu, C.-H. Doh, S.-M. Lee, Enhancement of ionic conductivity of composite membranes for all-solid-state lithium rechargeable batteries incorporating tetragonal {Li}7La3Zr2O12 into a polyethylene oxide matrix, *J. Power Sources*. 274 (2015) 458–463. <https://doi.org/10.1016/j.jpowsour.2014.10.078>.
- [3] J. Zhang, N. Zhao, M. Zhang, Y. Li, P.K. Chu, X. Guo, Z. Di, X. Wang, H. Li, Flexible and ion-conducting membrane electrolytes for solid-state lithium batteries: {Dispersion} of garnet nanoparticles in insulating polyethylene oxide, *Nano Energy*. 28 (2016) 447–454. <https://doi.org/10.1016/j.nanoen.2016.09.002>.
- [4] F. Chen, D. Yang, W. Zha, B. Zhu, Y. Zhang, J. Li, Y. Gu, Q. Shen, L. Zhang, D.R. Sadoway, Solid polymer electrolytes incorporating cubic {Li}7La3Zr2O12 for all-solid-state lithium rechargeable batteries, *Electrochim. Acta*. 258 (2017) 1106–1114. <https://doi.org/10.1016/j.electacta.2017.11.164>.
- [5] J. Zheng, H. Dang, X. Feng, P.-H. Chien, Y.-Y. Hu, Li-ion transport in a representative ceramic–polymer–plasticizer composite electrolyte: {Li} 7 {La} 3 {Zr} 2 {O} 12 – polyethylene oxide–tetraethylene glycol dimethyl ether, *J. Mater. Chem. A*. 5 (2017) 18457–18463. <https://doi.org/10.1039/C7TA05832B>.
- [6] M. Keller, G.B. Appetecchi, G.-T. Kim, V. Sharova, M. Schneider, J. Schuhmacher, A. Roters, S. Passerini, Electrochemical performance of a solvent-free hybrid ceramic-polymer electrolyte based on Li7La3Zr2O12 in P(EO)15LiTFSI, *J. Power Sources*. 353 (2017) 287–297. <https://doi.org/10.1016/j.jpowsour.2017.04.014>.
- [7] F. Langer, I. Bardenhagen, J. Glenneberg, R. Kun, Microstructure and temperature dependent lithium ion transport of ceramic–polymer composite electrolyte for solid-state lithium ion batteries based on garnet-type {Li}7La3Zr2O12, *Solid State Ionics*. 291 (2016) 8–13. <https://doi.org/10.1016/j.ssi.2016.04.014>.
- [8] S.H.-S. Cheng, K.-Q. He, Y. Liu, J.-W. Zha, M. Kamruzzaman, R.L.-W. Ma, Z.-M. Dang, R.K.Y. Li, C.Y. Chung, Electrochemical performance of all-solid-state lithium batteries using inorganic lithium garnets particulate reinforced {PEO}/{LiClO}4 electrolyte, *Electrochim. Acta*. 253 (2017) 430–438. <https://doi.org/10.1016/j.electacta.2017.08.162>.
- [9] J. Zagórski, J.M. López Del Amo, M.J. Cordill, F. Aguesse, L. Buannic, A. Llordés, Garnet-Polymer Composite Electrolytes: New Insights on Local Li-Ion Dynamics and Electrodeposition Stability with Li Metal Anodes, *ACS Appl. Energy Mater.* 2 (2019) 1734–1746. <https://doi.org/10.1021/acsaem.8b01850>.

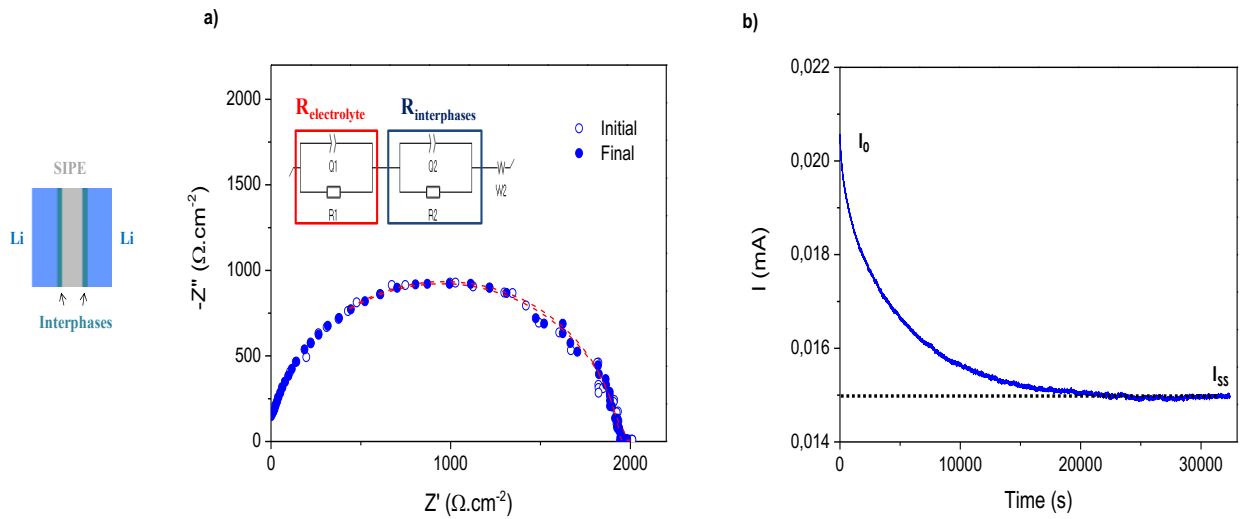


Fig.S5. Transference number determination for SIPE  
 (a) EIS spectra and simulated data from equivalent circuit modeling  
 (b) Intensity decay after polarization

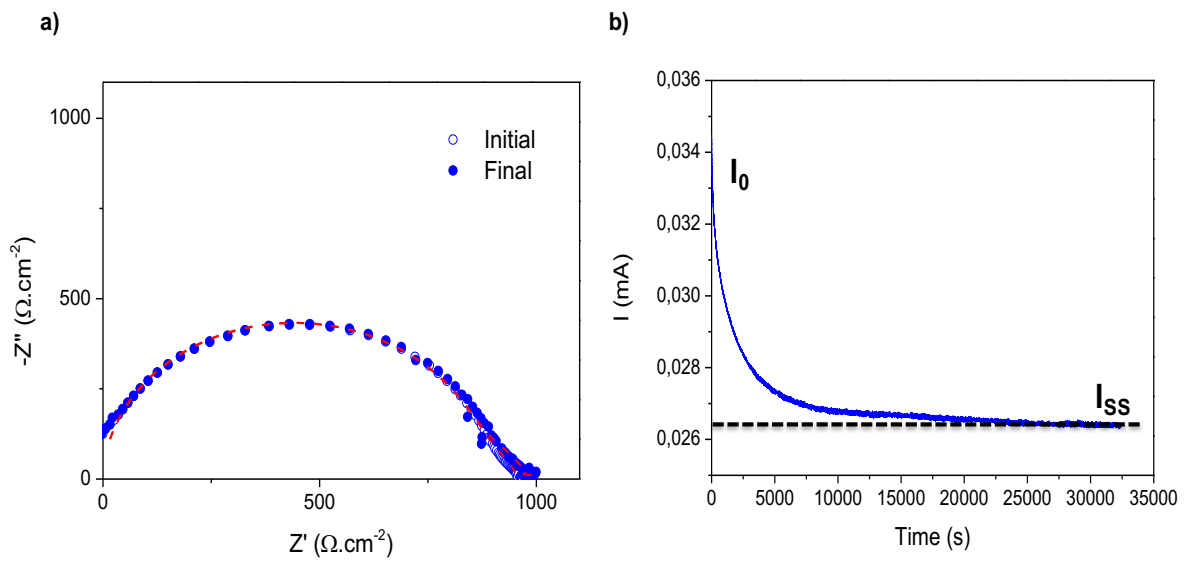


Fig.S6. Transference number determination for HSIPE-9  
 (a) EIS spectra and simulated data from equivalent circuit modeling  
 (b) Intensity decay after polarization

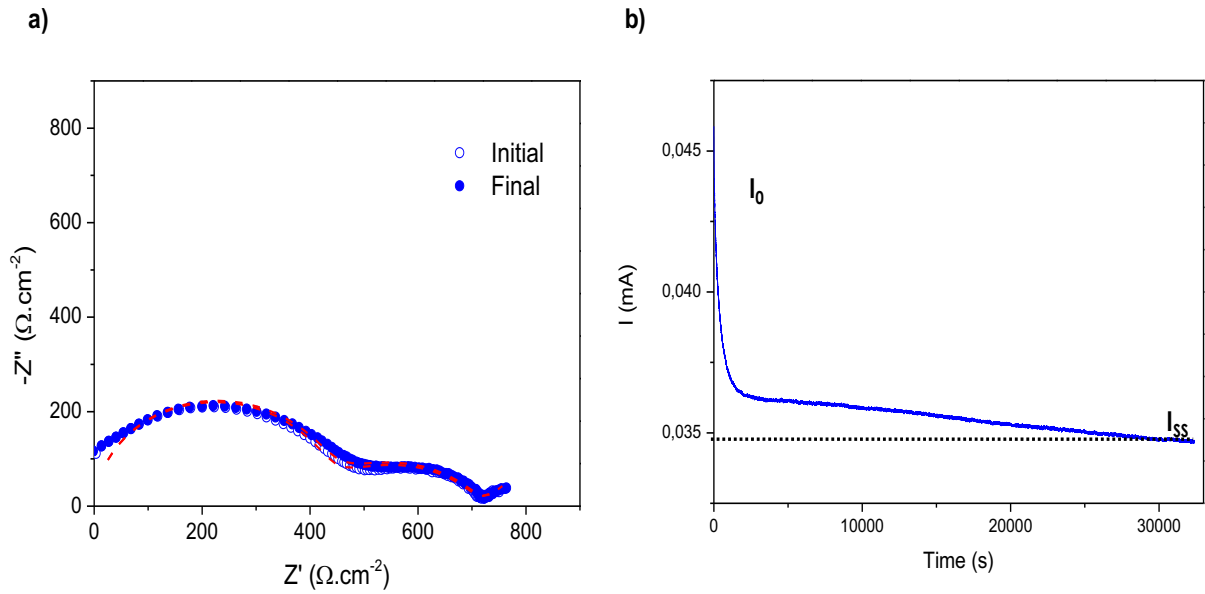


Fig.S7. Transference number determination for HSIPE-26  
 (a) EIS spectra and simulated data from equivalent circuit modeling  
 (b) Intensity decay after polarization

**Table S8:** Ionic conductivities for the different pristine and hybrid compositions

Compositions	$\sigma_{25^{\circ}\text{C}}$ ( $10^{-4}$ S.cm $^{-1}$ )	$\sigma_{50^{\circ}\text{C}}$ ( $10^{-4}$ S.cm $^{-1}$ )	$\sigma_{70^{\circ}\text{C}}$ ( $10^{-4}$ S.cm $^{-1}$ )
SIPE	0.48	0.95	1.62
HPE-26	0.11	0.22	0.34
HSIPE-26	1.17	2.67	4.41
HSIPE-9	0.88	2.04	3.38
DIPE	21	42	106
HDIPE-26	14.2	28.9	48.4

**Table S9:**  $^7\text{Li}$   $T_1$  relaxations times obtained by saturation recovery at 22°C

Samples	SIPE	HSIPE-26	HSIPE-9	DIPE	HDIPE-26
Narrow (s)	0.23	1.6	0.25	0.26	1.03
Broad (s)	-	15.8	6.9		15.0

**Table S10:**  $^7\text{Li}$  diffusion coefficients at various temperatures

Composition	$D_{70^\circ\text{C}}$ ( $10^{-12} \text{ m}^2.\text{s}^{-1}$ )	$D_{50^\circ\text{C}}$ ( $10^{-12} \text{ m}^2.\text{s}^{-1}$ )	$D_{22^\circ\text{C}}$ ( $10^{-12} \text{ m}^2.\text{s}^{-1}$ )
SIPE	13.1	6.77	2.05
HSIPE-26	17.1	7.03	2.94
HSIPE-9	15.3	8.68	2.78
DIPE	27.7	15.5	5.44
HDIPE-26	23.8	15.2	5.81

**Table S11:**  $^{19}\text{F}$  diffusion coefficients at various temperatures

Composition	$D_{70^\circ\text{C}}$ ( $10^{-11} \text{ m}^2.\text{s}^{-1}$ )	$D_{50^\circ\text{C}}$ ( $10^{-11} \text{ m}^2.\text{s}^{-1}$ )	$D_{22^\circ\text{C}}$ ( $10^{-11} \text{ m}^2.\text{s}^{-1}$ )
DIPE	16.4	10	3.91
HDIPE-26	10.3	5.65	1.98

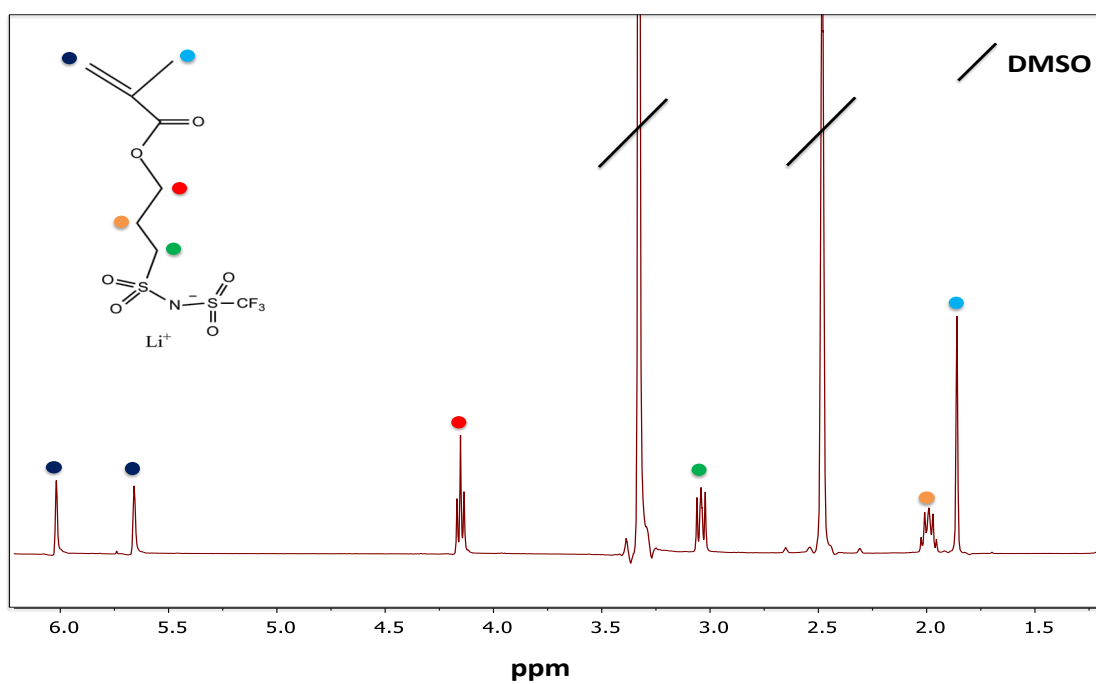


Fig.S12.  $^1\text{H}$  NMR spectrum of single ion monomer LiMTFSI

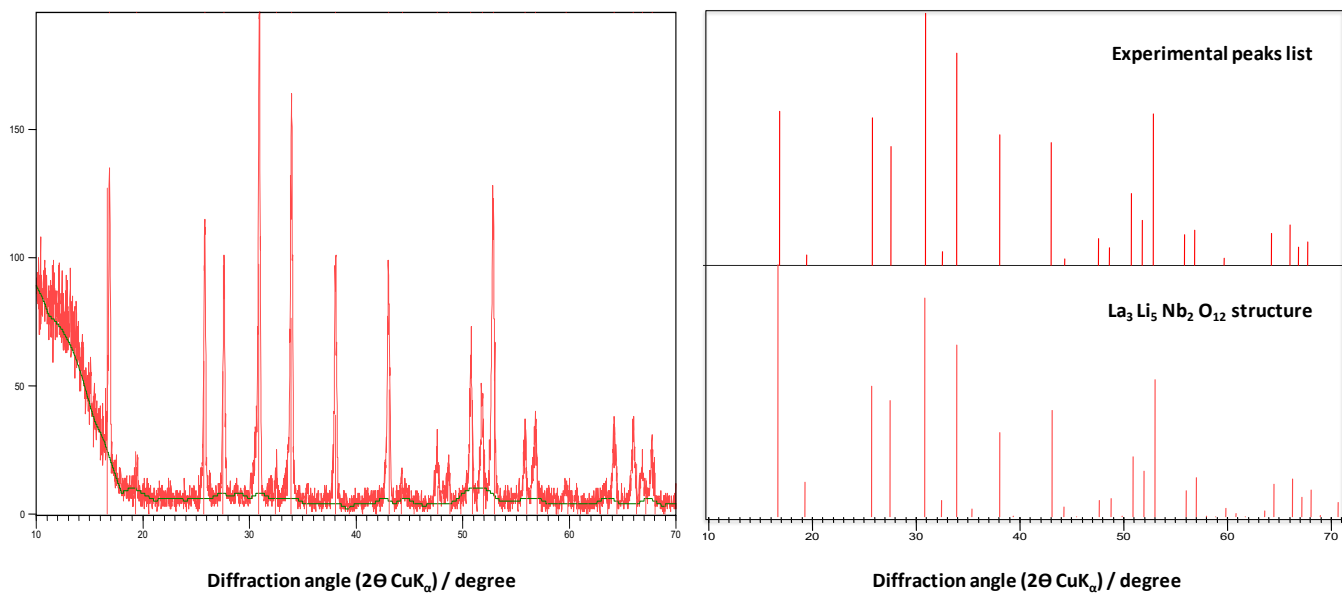


Fig.S13. XRD pattern of LLZO particles and their comparison with the crystalline  $\text{La}_3\text{Li}_5\text{Nb}_2\text{O}_{12}$  structure (Ia3d)